© UM, Guimarães, 2013

Creep Behavior of Concrete Elements Strengthened with NSM CFRP Laminate Strips under Different Environmental Conditions

J. Sena-Cruz[1], P. Silva[2], P. Fernandes[3], M. Azenha[4], J. Barros[5], C. de Sousa[6], F. Castro[7], T. Teixeira[8]

[1]ISISE, Universisty of Minho, Azurém, Guimarães, Portugal, jsena@civil.uminho.pt
[2]ISISE, Universisty of Minho, Azurém, Guimarães, Portugal, patricia.silva@civil.uminho.pt
[3]ISISE, Universisty of Minho, Azurém, Guimarães, Portugal, pfernandes@civil.uminho.pt
[4]ISISE, Universisty of Minho, Azurém, Guimarães, Portugal, miguel.azenha@civil.uminho.pt
[5]ISISE, Universisty of Minho, Azurém, Guimarães, Portugal, barros@civil.uminho.pt
[6]ISISE, Universisty of Minho, Azurém, Guimarães, Portugal, christoph@civil.uminho.pt
[7]CT2M, Universisty of Minho, Azurém, Guimarães, Portugal, fcastro@dem.uminho.pt
[8]ISISE, Universisty of Minho, Azurém, Guimarães, Portugal, tiago.teixeira@civil.uminho.pt

Keywords: NSM; CFRP; Flexural Strengthening; Slabs; Creep Test; Aging tests.

SUMMARY
The present work intends to contribute for the knowledge on the long-term deformational performance of concrete structures strengthened with the near-surface mounted (NSM) technique. For that purpose a wide experimental program has been initiated using beam pullout and slab specimens submitted to sustained loads under the following environmental conditions: (i) 20ºC temperature and 55% relative humidity; (ii) immersed in water tank at 20ºC with 0% of chlorides; (iii) immersed in water tank at 20ºC with 2.5% of chlorides; (iv) submitted to wet/dry cycles at 20ºC with 2.5% of chlorides. The slabs are continuously monitored in terms of mid-span vertical deflection and strains (in concrete, CFRP laminate strip and steel reinforcements), whereas for the case of the beam pullout specimens monitoring includes the free and loaded end slips and strain in CFRP laminate strip. The present paper summarizes the preliminary results.

1. INTRODUCTION

In the last decade, the near-surface mounted (NSM) technique using fiber reinforced polymers (FRP) has been adopted to increase the load carrying capacity of concrete members [1]. With this technique, the FRP reinforcing elements, whose cross-section can be round, square, rectangular or oval, are introduced into saw cut grooves opened on the concrete cover of the concrete members to be strengthened. These grooves are previously filled with a structural epoxy adhesive.

The NSM technique became a real alternative to other techniques, such as the externally bonded reinforcement (EBR), due to several main advantages [1]: reduction of amount of site installation work; less proneness to debonding; easier to anchor into adjacent members to prevent debonding failures; higher strengthening effectiveness; more protected by the concrete cover and so less exposed to accidental impacts/damages, fire, and acts of vandalism; the visual appearance of the strengthened structure is virtually unchanged; in some cases, the ultimate strength of FRP can be reached.

In spite of significant developments that have been carried out, when compared with the EBR, the existing knowledge on the NSM reinforcement is much more limited. However, normative institutions, such as the American Concrete Institute (ACI) [2] or Standards Australia (SA) [3], issued

design guidelines for the flexural strengthening with the NSM technique. Literature related to long-term behavior and durability of NSM strengthening systems is extremely scarce [4-6]. Even though these works that have been done with a limited number of specimens, it was clear that aggressive actions such as elevated temperature exposure, salt water spray or wet-dry cycles yielded non-negligible degradation in the ultimate strength compared with reference prototypes. However, this decrease did not surpass 11%. Since the NSM is an emerging technique, these subjects need to be addressed. In this context, the R&D project "CutInDur - Long-term structural and durability performance of concrete elements strengthened with the NSM technique" funded by the Portuguese Foundation for Science and Technology aims to contribute for increasing the knowledge in this area. Figure 1 gives an overview of this project. Two different scales are used to do the study: mesoscale and full scale by using pullout and slab specimens, respectively. The bond behavior is evaluated with the former specimens, whereas the overall structural behavior is assessed by the latter ones. The effect of different environmental actions is studied, encompassing effects such as moisture, freeze-thaw, wet-dry and thermal cycles. The chemical action considered is the effect of chlorides. Lastly, two types of loading are considered: sustained (creep) and fatigue loads.

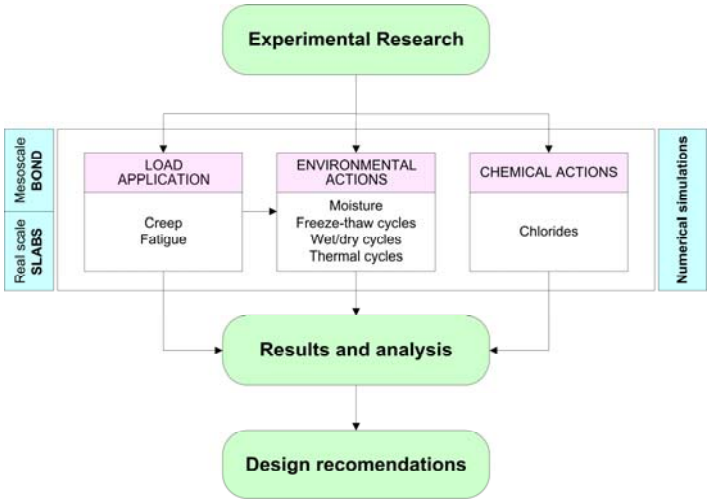

Figure 1: Flowchart of the R&D project CutInDur

The present paper will focus on the creep behavior of concrete elements strengthened with NSM CFRP laminate strips under different environmental conditions. The description of the experimental program, preparation of specimens and loading, as well as preliminary results are presented in detail in the following section of this paper.

2. EXPERIMENTAL PROGRAM

The creep behavior of concrete elements strengthened with NSM CFRP laminate strips under different environmental conditions will be assessed by using 8 beam pullout specimens and 8 slab specimens within an experimental program summarized in Table 1. Three environmental actions are considered: specimens immersed in water tank at 20ºC with 0% of chlorides (Series S2); specimens immersed in water tank at 20ºC with 2.5% of chlorides (Series S3); and specimens submitted to a wet/dry cycles with water at 20ºC and 2.5% of chlorides (Series S4). Additionally, reference specimens are kept in the lab environment with an average 20ºC temperature and 55% relative humidity (Series S1). The percentage of chlorides was based on the ASTM D1141-98 [7], which recommends 24.53 g of NaCl per liter of water. Half of the specimens will be submitted to these environmental actions during 360 days, whereas the other half will continue during more 360 days. At the end of each aging test, the specimens will be monotonically tested up to failure. Finally, to define the creep load level reference specimens were tested up the failure (DPT, BPT, REF and STR). The code names given to the test series consist on alphanumeric characters separated by underscores (see Table 1). The first string indicates the specimen type (BP and SL). The second string defines the environmental action (REF,

PW, CW and WD). Finally, the last string indicates the number of days that the specimen will be submitted to the environmental action.

Table 1: Experimental program.

Series	***Environmental action***	***Beam pullout specimens***	***Slab specimens***
S0	Lab environment	DPT* and BPT*	REF* and STR*
S1	Lab environment	BP_REF360 BP_REF720	SL_REF360 SL_REF720
S2	Prototypes immersed in pure water at 20ºC	BP_PW360 BP_PW720	SL_PW360 SL_PW720
S3	Prototypes immersed in water at 20ºC with 2.5% of chlorides	BP_CW360 BP_CW720	SL_CW360 SL_CW720
S4	Prototypes submitted to wet/dry cycles with water at 20ºC with 2.5% of chlorides	BP_WD360 BP_WD720	SL_WD360 SL_WD720

* These specimens were tested before the creep tests have started.

2.1 Materials and material characterization

The adopted materials are: concrete, steel, adhesive and CFRP laminate strip. Physical, chemical and mechanical characteristics are assessed in order to understand the evolution of the system under the different aging tests.

Concrete

Only one batch was used to cast all the specimens (3.6 m^3). The supplied concrete has the following properties: concrete strength class - C25/30, according to Eurocode 2 [8]; maximum aggregate size - 12 mm; cement strength class - CEM 42.5 (type II); exposure class XC4, according to Eurocode 2 [8]. Five cylindrical concrete specimens with 150 mm of diameter and 300 mm height were tested at 28-days of concrete age to evaluate the modulus of elasticity and the compressive strength according to the recommendations LNEC E397-1993:1993 [9] and NP EN 12390-3:2011 [10], respectively. Before starting the evaluation of the modulus of elasticity one additional cylinder (sixth) was tested up to failure in order to have an idea about the concrete compressive strength. The obtained compressive strength f_{cm} was 36.0 MPa, with a coefficient of variation (CoV) of 3.9%; the average Young's modulus was of 28.4 GPa (CoV=5.8%).

CFRP laminate strips

The CFRP laminate strip with a rectangular cross-section with 10×1.4 mm^2 used in the present experimental program is produced by S&P® Clever Reinforcement Company and is provided in rolls of 50 -100 m length. The laminate has the trademark CFK 150/2000 and is composed of unidirectional carbon fibers agglutinated by an adhesive. Young's modulus and tensile strength evaluation of the CFRP laminated were performed according to ISO 527-5:1997(E) [11]. From five tested specimens, a Young's modulus and tensile strength of 178 GPa (CoV=0.6%) and 2858 MPa (CoV=2.4%) were obtained, respectively. In order to evaluate the CFRP degradation under different environmental conditions, scanning electron microscope (SEM) observations have been done for reference. Figure 2(a) shows the micro-structure of the CFRP laminate strip before being submitted to aging tests. At this micro-scale several carbon fibers can be seen with a non-structured distribution and with several spaces filled by the epoxy vinylester resin.

Epoxy adhesive

A thixotropic grey two-component (A and B) epoxy resin produced by the same supplier was used to bond the CFRP laminate strips to concrete. This adhesive has the trademark "S&P Resin 220". Tests performed by Michels *et* al. [12] have revealed that this epoxy cured at room temperature, at 7-days of age, has an average Young's modulus and a tensile strength of 7.7 GPa (CoV=3.1%) and 20.7 MPa (CoV=9.9%), respectively. Scanning electron microscope (SEM) with energy dispersive spectroscopy

was used to determine the chemical composition of the constituents of the epoxy (see Figure 2(b)). From this analysis some mineral fillers, such as quartz, feldspar (SlAlK), barite (SBaO) and other silicates were observed.

Steel reinforcement
Tension tests according to NP EN 10002-1:1990 [13] were performed to assess to the mechanical characteristics of the steel reinforcement (Ø6). The average value of the modulus of elasticity, hardening modulus and ultimate strength were, respectively, 212.2 GPa (CoV=6.3%), 0.7 GPa (CoV=6.6%) and 733.0 MPa (CoV=1.0%).

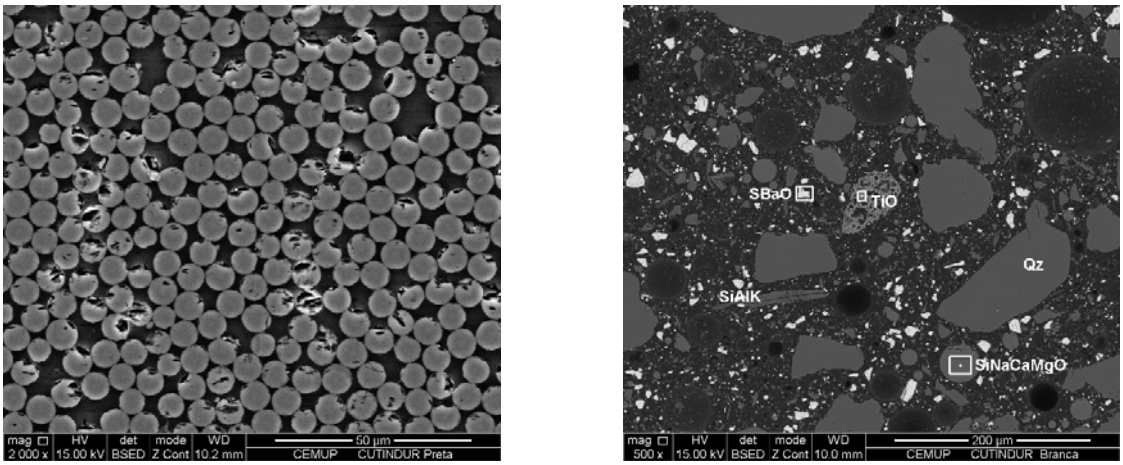

(a) (b)

Figure 2: SEM observations - (a) CFRP laminate and (b) epoxy adhesive.

2.2 Specimens and test configuration
Figure 3 shows the geometry and test configuration adopted for the beam pullout specimens. The specimen is composed by two concrete blocks (A and B) of equal size, each with dimensions 150×200×385 mm^3. In each block 5 stirrups composed by rebars of 6 mm diameter (Ø6) were used to avoid shear failure. Additionally, these blocks were longitudinally strengthened with 2Ø8 at the bottom and 2Ø8 at the top. The concrete cover was 20 mm. The blocks are interconnected by a steel hinge located at mid-span in the top part, and also by the CFRP laminate strip (1.4 mm thick and 10 mm wide) fixed at the bottom. The bond test region was located in the bottom part of block A, with the fixed bonded length (L_b) equal to 60 mm. The bond length started at 100 mm distance from the extremity of the block to avoid premature splitting failure in the concrete ahead the loaded-end. On block B, the bond length was higher (335 mm) as this was not the side of the specimen to be tested. The instrumentation of the beam tests up to the failure consisted on the use of two LVDTs, a strain gauge and a load cell. The LVDT2 is used to control the test, at 2 μm/s slip rate, and simultaneously to assess the slip at the loaded-end, s_l, while the LVDT1 is used to measure the slip at the free-end, s_f. The value of s_l is obtained subtracting the elastic deformation of the CFRP between A and B to the records of LVDT2 (see Figure 3). The applied force F is registered by a load cell placed between the steel plate and the actuator. A strain gauge, glued on the CFRP surface placed at the mid-span of the specimen, measured the strains during the test for the evaluation of the pullout force (F_l), taking into account the modulus of elasticity and the cross sectional area of the CFRP laminate strip. It should be remarked that during the creep aging tests only the strains, displacements in the LVDT2 and applied force are measured.

In addition to the beam pullout tests, direct pullout tests are included in the present experimental program. However, these specimens are not part of the sustained load experiments. Figure 4 shows the geometry and test configuration of the direct pullout tests. The specimen's geometry consisted of cubic concrete blocks of 200 mm edge. To avoid premature failure due to the formation of a concrete fracture cone at the loaded end, bond lengths started 100 mm away from the top. A 20 mm thick steel

plate was placed at the top of the concrete block to assure negligible vertical displacements at the top during the pullout test. Four M10 threaded rods fixed this steel plate to the stiff base. A torque moment of 30 N×m was applied to fasten these rods. This torque moment induces an initial compressive stress state on the concrete block of about 2.0 MPa. The instrumentation of the specimens consisted of two variable differential transducer (LVDTs), as shown in Figure 4, and a load cell. LVDT1 records the relative displacement between concrete and the CFRP laminate at the top of the concrete block (100 mm apart from the loaded end section), while the LVDT2 is used to measure the slip at the loaded-end, s_l. The tests are controlled by another LVDT placed between the actuator and the grip, at rate of 2 μm/s. The applied force, F, is registered by a load cell placed between the grip and the actuator.

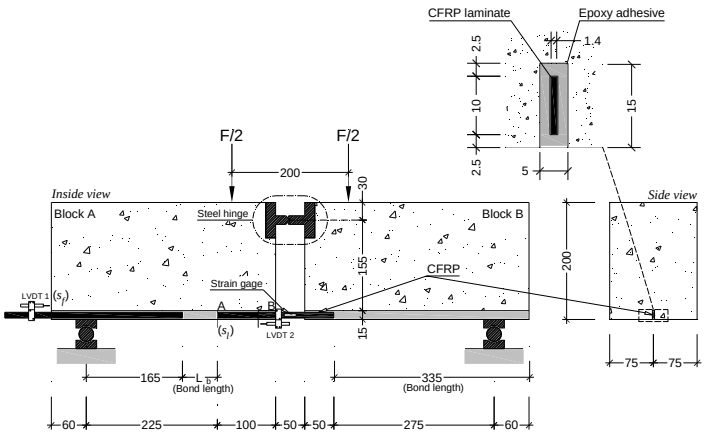

Figure 3: Beam pullout specimens: geometry and test configuration. Note: all units in [mm].

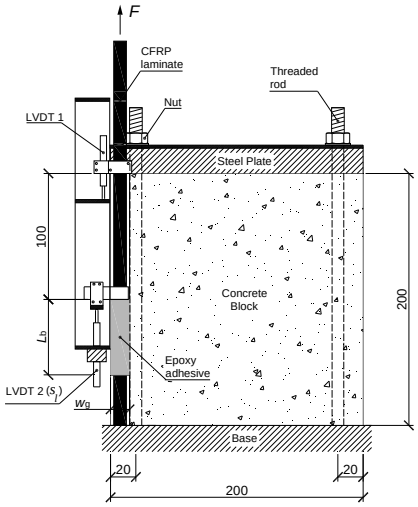

Figure 4: Direct pullout specimens: geometry and test configuration. Note: all units in [mm].

The cross-section geometry and reinforcement detailing, as well as the instrumentation and test configuration of the slabs are presented in Figure 5. The slabs are 2000 mm long, 300 mm wide and 80 mm thick. The longitudinal reinforcement is composed by 4Ø6, which corresponds to a longitudinal reinforcement ratio, ρ_l, equal to 0.47%. The flexural strengthening solution is composed by 3 CFRP laminate strips. The corresponding equivalent longitudinal reinforcement ratio is 0.68%. The instrumentation of the slab tests up to failure includes LVDTs, load cell and strain gauges. Five LVDTs measure the deflection along the slab's longitudinal axis, whereas the load cell records the applied vertical force. Five strain gauges (SG1 to SG5) are glued on the lateral surface of the intermediate CFRP to measure the strains in distinct sections. Two additional strain gauges (not included in the drawing Figure 5) are used to record the strains in the longitudinal reinforcement and concrete at the top fiber of the cross-section mid-span. In the tests up to failure, the internal displacement transducer of the servo-control equipment is used to control the test at 20 μm/s of deflection rate. During the creep aging tests only the strains, the deflection in the LVDT3 and applied force are measured. In addition to the LVDT3, one mechanical dial gage located at the opposite lateral face of the midspan slab was used. The main objective of this strategy is to have a redundant system for reading the midspan deflection.

All previously referred tests up to failure are performed with servo-controlled equipments, whereas the sustained load testing is made with gravity loads (mixed concrete/steel profiles and rock blocks).

2.3 Preparation of specimens

The preparation of the strengthened specimens required several steps, mainly: (i) opening the grooves with a saw cut machine; (ii) gluing strain gauges on the FRP and rebar surfaces; (iii) cleaning the grooves with compressed air and the laminates with acetone; (iv) preparation of the adhesive

according to the technical data sheet of the supplier; (v) application of the adhesive on the groove and lateral surfaces of the laminate; (vi) introducing carefully the laminate into the groove; (vii) level the surface. After opening the grooves, several measurements were done to assess the real grooves' geometry. From these measurements a width and depth of 5.47 mm (CoV=1.82%) and 15.59 mm (CoV=2.16%) were obtained, respectively. The strengthening of the specimens occurred at about 75 days after concreting. At this moment the opened grooves were completely dry and clean. The strengthening was performed in the interior of the lab with an average temperature of about 25ºC and 42% of relative humidity.

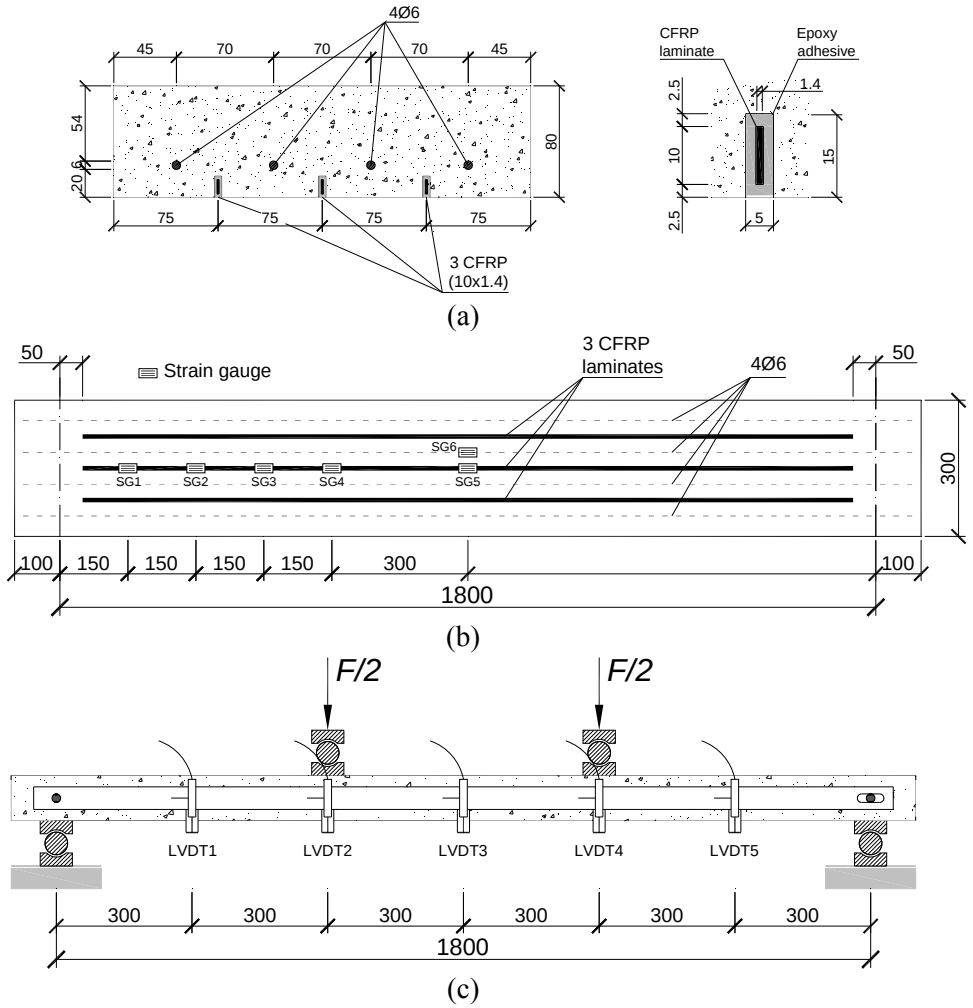

Figure 5: Slab specimens: (a) Cross-section geometry and reinforcement detailing; (b) Longitudinal geometry, reinforcement detailing and gauge instrumentation; (c) Test configuration. Note: all units in [mm].

3. RESULTS

Before starting the creep studies under different environmental conditions, monotonic tests were performed for both beam pullout and slab specimens up to failure (see Table 1). As previously referred, these tests had the main objective of evaluating the load carrying capacity of each specimen type and in order to define the creep load level (assumed equal at about 1/3 of its ultimate load). Then the creep load was applied in two different steps. In the ambit of the present work results of the monotonic tests up to the failure are presented, as well as the preliminary results in terms of deflection for the applied sustained load. Since this an ongoing research project, the effect of the different environmental conditions on creep behavior is not presented here.

3.1 Monotonic tests - Slabs

Two monotonic tests with slabs were carried: one unstrengthened slab (REF), and another one strengthened (STR) with the solution described in Section 2.1. The tests were performed with the specimens with 190 days of age. At this time the average concrete compressive strength in cylinders was 49.64 MPa.

Table 2 presents the results obtained in terms of midspan deflection and applied load for crack initiation (δ_{cr}, F_{cr}), yield initiation of the longitudinal reinforcements (δ_y, F_y), and maximum load (δ_{max}, F_{max}). This table also presents the ductility index (μ) reached in each test, defined as the δ_{max} / δ_y ratio. The failure mode is also indicated. Figure 6 presents the relationship between the applied load and the midspan deflection for both slabs (REF and STR). Figures 7 and 8 show the evolution of steel, concrete and CFRP strains with the applied load, respectively.

Table 2: Main results obtained in monotonic tests.

Slab	Crack initiation		Yielding		Ultimate		μ	Failure mode
	δ_{cr} [mm]	F_{cr} [kN]	δ_y [mm]	F_y [kN]	δ_{max} [mm]	F_{max} [kN]		
REF	1.03	2.57	25.11	11.42	52.80	12.03	2.10	CC
STR	1.47 (42.7%)	3.89 (51.4%)	32.92 (31.1%)	21.04 (84.2%)	86.30 (63.4%)	31.63 (162.9%)	2.62 (24.8%)	CC

Notes: the values between parentheses are the variation of the corresponding parameter when compared with the REF slab; CC – Concrete crushing.

In the F-δ curves the expected three branches corresponding to the three stages with distinct slopes are clearly identified (see Figure 6): stage I – uncracked concrete; stage II – cracked concrete; stage III – cracked concrete with the steel reinforcement yielded. The slope variations from stage I to II and II to III for the REF slab were -87% and -92%, while in the STR slab were -84% and -56%. The smaller variation observed in the STR slab from stage II to III was expected due to the CFRP reinforcement linear behavior up to failure, contributing for the increment of the load carrying capacity of structural element when the steel reinforcement yields. The yielding initiation registered by the strain gauges glued to the steel bars started at about 3.6‰ and 3.8‰ for the REF and STR slabs, respectively (see Figure 7). These values are quite close to the expected one (about 3.3‰ – see also Section 2.2). At the maximum load the registered concrete strains in the REF and STR slabs were of about 3.8‰ and 4.8‰, respectively. Since both specimens failed by concrete crushing (CC) at the top part of the slab in the midspan region, high concrete strain values were expected. It is also noticeable that the level of strengthening efficiency was quite high. In fact the CFRP strains reached 12‰ (see Figure 8), which is a common value in NSM systems and twice as large as the usual values reported for the EBR technique [14].

The average bond stress between two consecutive strain gauges *i* and *j*, τ_m^{ij}, can be evaluated by using Eq. (1). In this equation E_f and A_f are the Young's modulus and the cross-sectional area of the CFRP; P is the perimeter of the contact surface between FRP and adhesive; L^{ij} is the distance between two consecutive strain gauges; and, finally, $\Delta\varepsilon_f^{ij}$ is the axial strain variation of strain gauges positioned at *I* and *j* sections.

$$\tau_m^{ij} = \frac{E_f \cdot A_f \cdot \Delta\varepsilon_f^{ij}}{P \cdot L^{ij}} \quad (1)$$

Figure 9 presents the relationship bewteen the total load and the average bond stress at different locations. As expected in the pure bending region, the average bond stress was marginal since the

bending moment is constant (SG4-5). At the ultimate load (F_{max}) the average bond stress at SG1-2, SG2-3 and SG3-4 locations had the approximate value of 3 MPa.

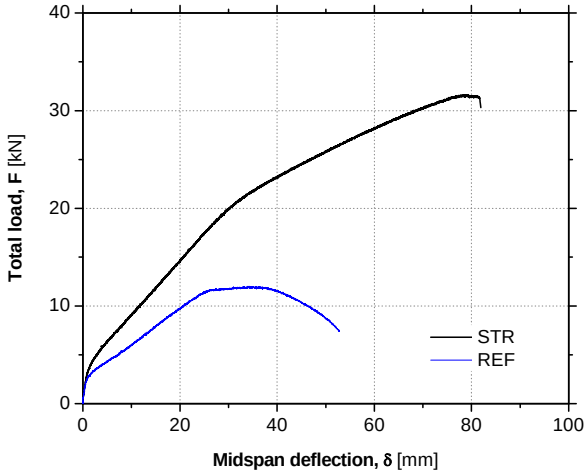

Figure 6: Relationship between total load and midspan deflection for REF and STR slabs.

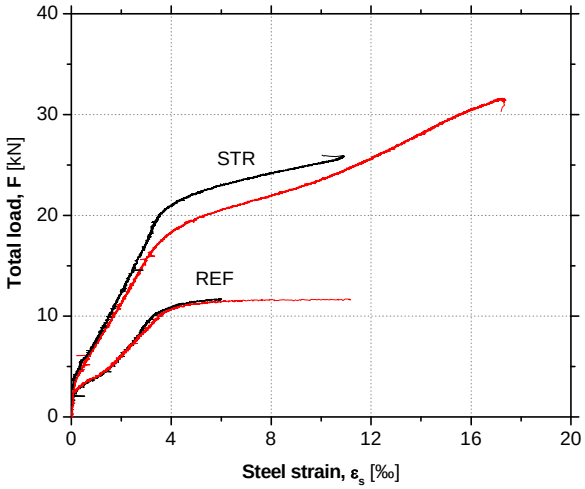

Figure 7: Total load *versus* steel strain at the slab mid-span.

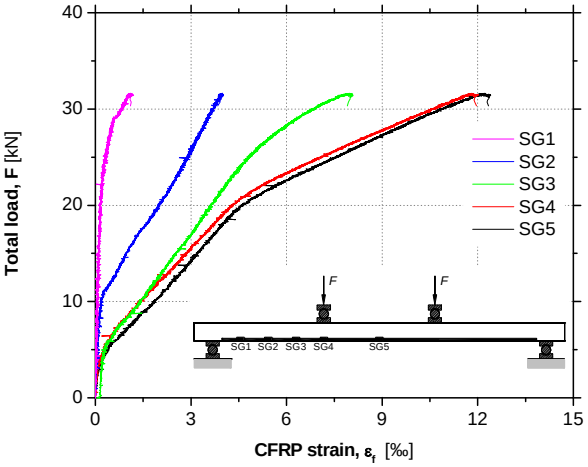

Figure 8: Total load *versus* CFRP strain at different locations (STR slab).

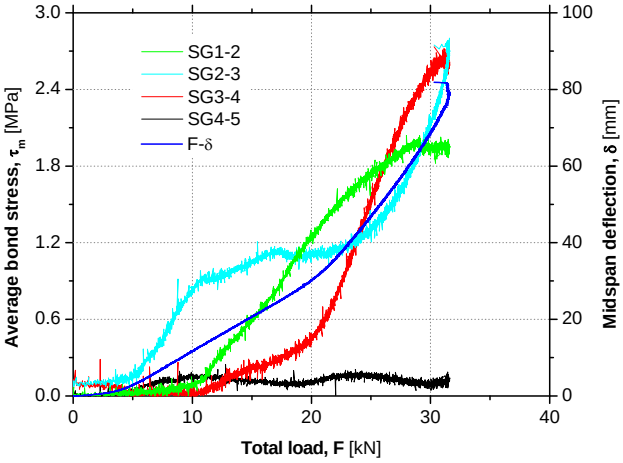

Figure 9: Total load *versus* average bond stress at different locations (STR slab).

3.2 Monotonic tests – Pullout specimens

Table 3 summarizes the main results obtained in pullout tests. In this table the meaning of each entity is the following: F_{fmax} is the maximum pullout force; F_{fu} is the CFRP tensile strength; s_{lmax} is the slip at the loaded end at the peak pullout force (F_{fmax}); s_{fmax} is the slip at the free end at the peak pullout force (F_{fmax}); $\tau_{max,av1}$ and $\tau_{max,av2}$ are the average bond strength at the CFRP-epoxy and concrete-epoxy interfaces, respectively, and are evaluated by $F_{fmax}/(P_f L_b)$ and $F_{fmax}/(P_g L_b)$, where P_f is the perimeter of the CFRP cross-section, P_g is the perimeter of the groove cross-section in contact with the adhesive and L_b is the bond length.

From this table it is possible to conclude that the maximum pullout force (F_{fmax}) obtained from both test configurations (BPT and DPT) is approximately equal. As expected, when $\tau_{max,av1}$ and $\tau_{max,av2}$ are compared, higher values were obtained in the former cases. With the exception of the DPT2 specimen, all the others failed by debonding at adhesive/laminate interface. Excluding the DPT2 specimen from DPT series (that failed prematurely), both series yielded to low values of the coefficient of variation for the force and stress variables. However, higher values were observed in the slip at free and loaded ends.

Figures 10 and 11 depict the relationships between pullout force and slip for BPT and DPT, respectively. In general, the F_l-s_l responses are firstly characterized by short linear branch with a significant slope value due to the chemical bond between the concrete/adhesive/CFRP. When this connection starts being damaged, the response becomes essentially nonlinear up to the peak load, due to the debonding process. In the specimen BPT2, after reaching the peak load, a softening branch was observed. In both BPT specimens similar behavior was observed. The F_l-s_f responses revealed that the debonding process at the free end region only starts for a load level close to the peak. In the DPT series similar maximum pullout forces were reached, with the exception of the DPT2 specimen where at about F_l=20 kN a significant portion of the CFRP laminate broke.

Table 3: Main results obtained in monotonic tests.

Specimen	F_{fmax} [kN]	F_{fmax} / F_{fu} [%]	$\tau_{max,av1}$ [MPa]	$\tau_{max,av2}$ [MPa]	s_{fmax} [mm]	s_{lmax} [mm]	**Failure mode**
BPT1	24.22	69.20	17.70	10.91	0.23	0.80	D
BPT2	24.03	68.66	17.57	10.82	0.15	0.70	D
BPT	24.13* (0.6%)	68.93* (0.6%)	17.64* (0.5%)	10.87* (0.6%)	0.19* (29.8%)	0.75* (9.4%)	-
DPT1	24.68	70.51	18.04	11.11	n/a	0.53	D
DPT2	21.14	60.40	15.45	9.52	n/a	0.64	F
DPT3	23.93	68.37	17.49	10.78	n/a	0.50	D
DPT4	24.15	69.00	17.65	10.88	n/a	0.62	D
DPT	24.25** (1.6%)	69.29** (1.6%)	17.73** (1.6%)	10.92** (1.6%)	-	0.55** (11.1%)	-

Notes: D=Debonding at adhesive/laminate interface; F=CFRP failure; The values between parentheses are the coefficients of variation.*Average values of BPT1 and BPT2 specimens; **Average values of DPT1, DPT3 and DPT4 specimens.

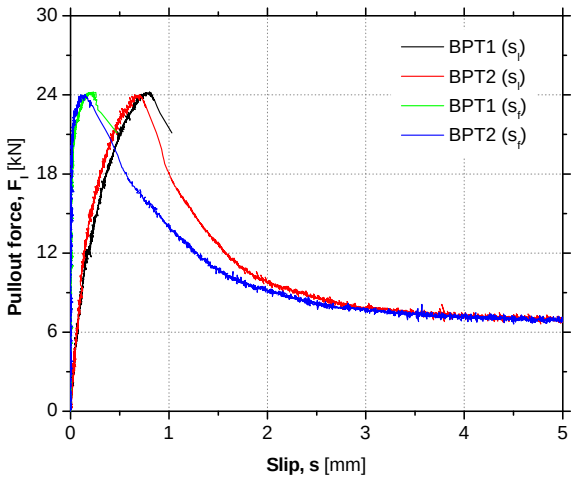

Figure 10: Pullout force *versus* free and loaded end slips for the beam pullout tests (BPT).

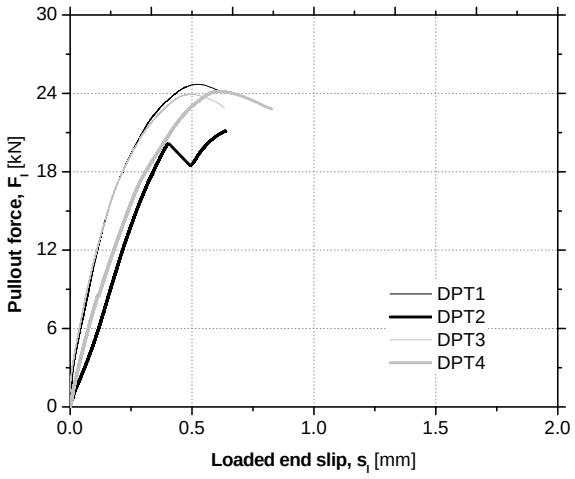

Figure 11: Pullout force *versus* loaded end slip for the direct pullout tests (DPT).

3.3 Creep tests – Slabs

For each slab Figure 12 shows the results of the ongoing creep tests in terms of the evolution of the deflection at midspan along time. The total creep load applied in each slab was 10 kN, which corresponds approximately to 1/3 of its corresponding ultimate load, as previously referred. This load was applied in distinct steps (L1 and L2). In the first one (L1), at about 40% of the total creep load was applied, which caused an instantaneous deflection of about 2 mm. The magnitude of this deflection is in agreement with the results obtained in the monotonic test of slab STR (see Figure 6). The maximum difference of the applied load for distinct slabs during step L1 was limited to 0.7 kN, which is sufficient to justify the different deflections observed. At the second load step (L2), suitable adjustments were made in order to assure the same load level for all the slabs. Nonetheless, a slight

difference between the midspan deflections for the 8 slabs remained. After applying the creep load of step L2, the average deflection at midspan was about 13 mm, against the 11.5 mm obtained in the monotonic test of STR slab (see Section 4.1).

Analysing the evolution of midspan deflection for steps L1 and L2 due to creep phenomena, the deflection changed from 2.0 mm to 3.2 mm (a variation of about 60%) in 78 days (duration of step L1) and from 13.2 mm to 15 mm (a variation of about 14%) in 55 days (duration of step L2), respectively.

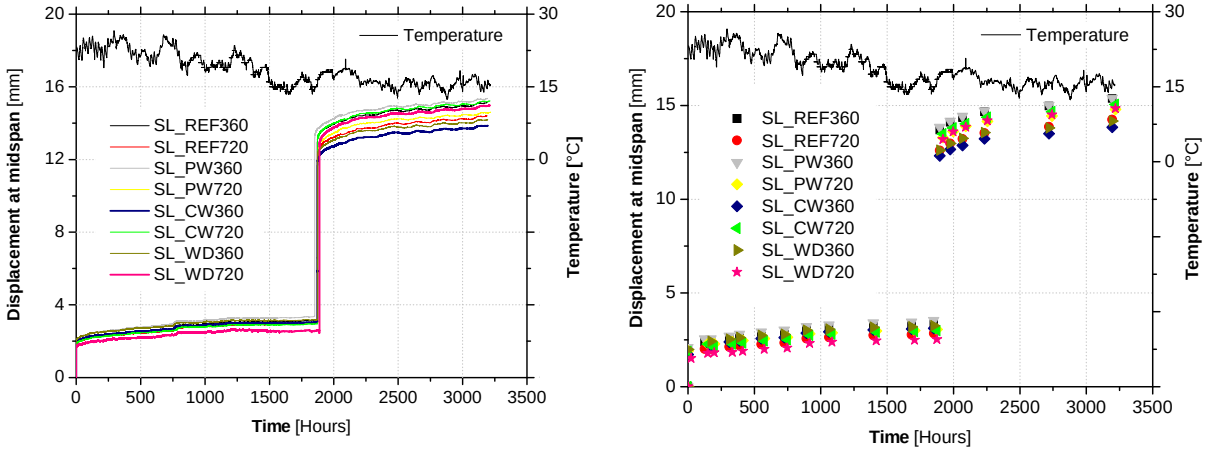

Figure 12: Displacement at midspan with time obtained by: (a) LVDT; (b) mechanical dials.

Crack width control is of considerable importance for structural diagnosis of concrete structures. Therefore, to assess the service life condition of the analysed slab specimens, localized visual inspections of the cracks that appear in the bottom surface of the slabs were conducted to verify if they comply with the serviceability requirements embodied in the European Standard Code [8]. The width of the cracks was assessed through a handheld USB microscope. The microscope was a VEHO VMS-004D, with a maximum magnification power of 400× and a native capturing resolution of 640×480 pixels. At the maximum magnification level, the field of measurement has about 1 mm by 0.75 mm, which means that each pixel corresponds to approximately 1.6 μm. To determine accurately the crack widths, the measurement procedure was based on the use of integrated circuits that were glued next to the cracks (as shown in Figure 13): the thickness of the markers engraved in every utilized circuit was previously measured (approximately 180 μm), which enabled calibration during measurements for every captured image. The crack width measurements were first taken at several points of the cracks with 20× magnification (see Figure 13a) and afterwards confirmed through localized measurements at 400× magnification, as illustrated in Figure 13b. The evolution of the crack width along the time can be seen Figure 14 for slabs SL_REF360, SL_CW360 and SL_WD360. The crack width ranges between 0.18 mm and 0.22 mm. These values are in the range of acceptable values according to Eurocode 2 [8], as the maximum admissible crack width of reinforced members is generally marked as 0.3 mm (for most environmental exposure conditions).

3.4 Creep pullout tests

Figure 15 presents the creep behavior of the beam pullout specimens. The total creep load (approximately 7 kN) applied to these specimens was defined in order to have the same level of CFRP strain existing in the slab creep tests. Like in the slabs, the total load is applied in two steps. The results presented in Figure 15 correspond to the first step, approximately 1.7 kN, which corresponds to 24% of the designed total creep load. It can be observed that the evolution of the slip measured by LVDT2 (see Figure 3) is highly affected by the temperature variation of the surrounding environment. The reference specimens, represented by black and green lines, installed out of the tanks, are less affected by this effect due to local microclimatic conditions. When the beam pullout results are compared with those from slabs, the temperature effect is more pronounced in the former, since the

CFRP laminates in slabs are totally surrounded by the adhesive and concrete. Finally, it should be remarked that the level of slip in the beam pullout specimens is very small (less than 0.1 mm).

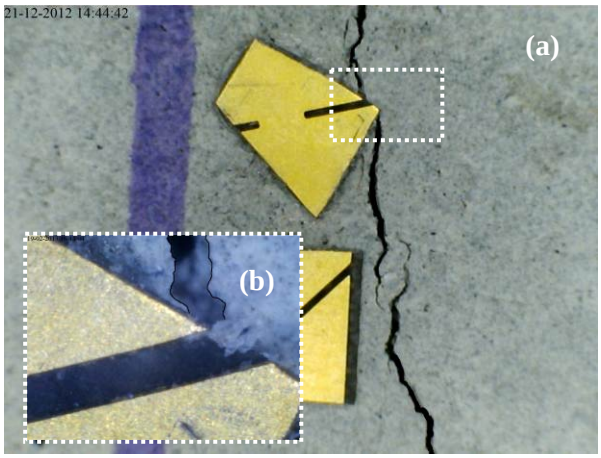

Figure 13: Images taken with microscope: (a) 20 times amplification; (b) 400 times amplification.

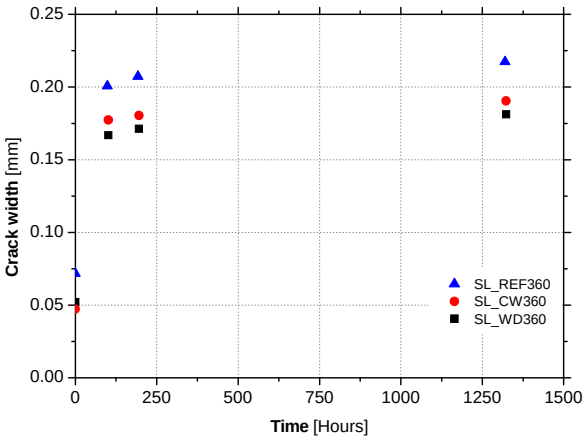

Figure 14: Crack width evolution with time for the monitored slabs.

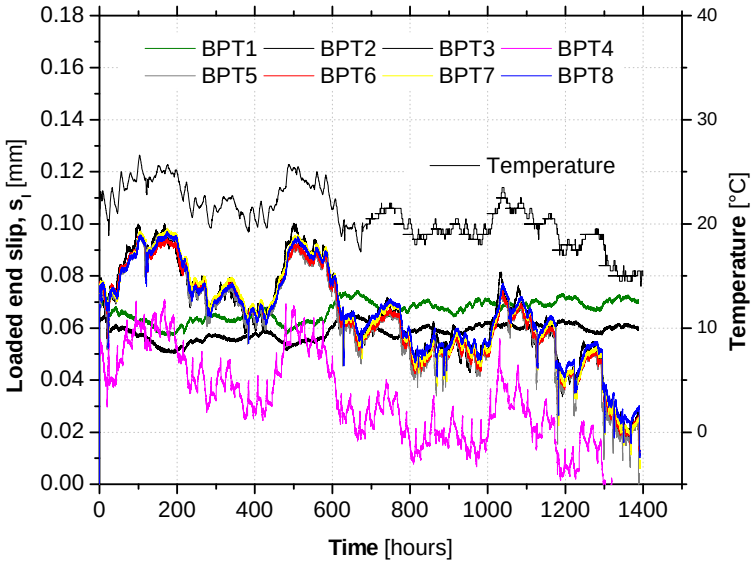

Figure 15: Creep behavior for the beam pullout specimens: loaded end slip *versus* time.

4. CONCLUSIONS

The present work has shown the general description and main up-to-date results of an ongoing research project whose main goal is to study the durability and long-term structural behavior of flexural reinforced concrete elements strengthened with NSM CFRP laminate strips. For that purpose, beam pullout and slab specimens were submitted to creep tests under different environmental conditions. The creep load applied to each slab (10 kN) was defined from the results obtained in a reference slab monotonically tested up to the failure. This value (10 kN) is approximately equal to 33% of the ultimate load of the reference slab. After 133 days, the average creep deformation for all the 8 studied slabs was about 3 mm, which corresponds at to about 20% of the total deflection. The crack widths are also monitored, being the current value at about 0.2 mm. Since, up to now, only the first creep load level was applied to the beam pullout tests (24% of the designed total creep load), the obtained results are dependent on the thermal conditions existing in the lab. The next step of the project is to immerse prototypes to pure water at 20ºC, immerse prototypes to water at 20ºC with 2.5% of chlorides and submit prototypes to wet/dry cycles with water at 20ºC with 2.5% of chlorides.

ACKNOWLEDGMENTS
This work is supported by FEDER funds through the Operational Program for Competitiveness Factors - COMPETE and National Funds through FCT - Portuguese Foundation for Science and Technology under the project CutInDur PTDC/ECM/112396/2009. The authors also like to thank all the companies that have been involved supporting and contributing for the development of this study, mainly: S&P Clever Reinforcement Ibérica Lda., Casais – Engenharia & Construção S.A., Artecanter - Indústria de Transformação de Granitos, Lda., Tecnipor - Gomes & Taveira Lda., Vialam – Indústrias Metalúrgicas e Metalomecânicas, Lda., Hilti Portugal-Produtos e Serviços, Lda., Novo Modelo Europa, S.A., Sika Portugal - Produtos Construção e Indústria, S.A., Cachapuz - Equipamentos para Pesagem, Lda. The second and third authors wishes also to acknowledge the grants SFRH/BD/89768/2012 and SFRH/BD/80338/2011, respectively, provided by FCT.

REFERENCES
[1] De Lorenzis, L., Teng, J.G. "Near-surface mounted FRP reinforcement: An emerging technique for strengthening structures." Composites: Part B, 38, 119-143, (2007).
[2] ACI 440F, "Guide for the design and construction of externally bonded FRP systems for strengthening concrete structures" report ACI 440.2R-08, American Concrete Institute, Farmington Hills, USA, 80 pp (2008).
[3] SA, "Design handbook for RC structures retrofitted with FRP and metal plates: beams and slabs", HB 305 – 2008, Standards Australia GPO Box 476, Sydney, NSW 2001, Australia, 76 pp, (2008).
[4] Burke, P.J. Low and High Temperature Performance of Near Surface Mounted FRP Strengthened Concrete Slabs. Master of Science, Queen's University (2008).
[5] Derias, M., El-Hacha R., Rizkalla, S. "Durability of various NSM FRP Strengthening Systems for RC Flexural Members", 5th International Conference on Advanced Composite Materials in Bridges and Structures (ACMBS-V), Winnipeg, Manitoba, Canada, 9 pp. (2008).
[6] Sena-Cruz, J.M.; Fernandes, P.; Silva, P.; Xavier, J.; Barros, J.; Coelho, M. "Bond behaviour of concrete elements strengthened with NSM CFRP laminate strips under wet-dry cycles" Bond in Concrete 2012, Brescia, Italy, 1023-1030, (2012).
[7] ASTM D1141-98. "Standard practice for the preparation of substitute ocean water" ASTM - American Society for Testing and Materials, (2003).
[8] EN 1992-1-1:2004. "Eurocode 2: Design of concrete structures - Part 1-1: General rules and rules for buildings" CEN - European Committee for Standardization, Brussels, 225 pp.
[9] LNEC E397-1993:1993. "Concrete - Determination of the elasticity Young modulus under compression." Portuguese specification from LNEC.
[10] NP EN 12390-3:2011. "Testing hardened concrete. Part 3: Compressive strength of test specimens." IPQ - Instituto Português da Qualidade, Caparica.
[11] ISO 527-5:1997. "Plastics — Determination of tensile properties — Part 5: Test conditions for unidirectional fibre-reinforced plastic composites." ISO - International Organization for Standardization, Genève, 11 pp.
[12] Michels, J.; Sena-Cruz, J.M.; Czaderski, C.; Motavalli, M. "Structural strengthening with prestressed CFRP strips with gradient anchorage", Composites for Construction Journal, (2013). Accepted for publication.
[13] NP EN 10002-1:1990 "Metallic materials. Tensile testing. Part 1: method of test (at ambient temperature)." IPQ - Instituto Português da Qualidade, Caparica, 34 pp.
[14] CNR-DT 200/2004 "Guide for the Design and Construction of Externally Bonded FRP Systems for Strengthening Existing Structures." CNR – Advisory Committee on Technical Recommendations for Construction, Italy, 154 pp, (2004).